Design and pilot testing of a 26-gauge impedance-electromyography needle in wild type and ALS mice

Seward B. Rutkove MD[1], Mai Le[2], Sophie A. Ruehr, BS[2], Janice A. Nagy PhD[1], Carson Semple, BS[1], and Benjamin Sanchez PhD[3*]

[1]Department of Neurology, Beth Israel Deaconess Medical Center, Harvard Medical School, Boston, MA, 02215, USA.

[2]Haystack Diagnostics, Inc, c/o M2D2, 110 Canal Street, 4th Floor, Lowell, MA 01854, USA

[3]Department of Electrical and Computer Engineering, University of Utah, Salt Lake City, UT, 84112, USA.

Number of words in Abstract: 241 (max 250)

Number of words in manuscript: 2127 (max 4000)

Address correspondence to:

*Benjamin Sanchez, PhD, Sorenson Molecular Biotechnology Building, 36 S Wasatch Drive, Office 3721, Salt Lake City, UT 84112. Tel: 801-585-9535. Email: benjamin.sanchez@utah.edu

Running title: Needle iEMG in WT and ALS mice

Ethical Publication Statement:

We confirm that we have read the Journal's position on issues involved in ethical publication and affirm that this report is consistent with those guidelines.

Disclosure of Conflicts of Interest:

Dr. Rutkove has equity in, and serves a consultant and scientific advisor to Myolex, Inc and Haystack Diagnostics, Inc., companies that design impedance devices for clinical and research use; he is also a member of the Myolex's Board of Directors. The companies also have an option to license patented impedance technology of which Dr. Rutkove is named as an inventor. Dr. Sanchez also holds equity and serves as scientific advisor in Haystack Diagnostics, Inc., and the company has an option to license patented needle impedance technology where the author is named an inventor. He also holds equity and serves as Scientific Advisory Board Member of Ioniq Sciences, Inc., a company that develops clinical impedance technology for early cancer detection. Dr. Sanchez serves as Scientific Advisory Board Member of B-Secur, Ltd., a company that develops wearable ECG and impedance technology. He consults for Myolex, Inc., the company has an option to license patented surface impedance technology where the author is named an inventor. Dr. Sanchez also serves as a consultant to Impedimed, Inc., a company that develops clinical impedance technology. The company patented impedance technology where the author is named an inventor. He also serves as consultant to Texas Instruments, Inc., Happy Health, Inc., and Analog Devices, Inc., companies that develop impedance related technology for consumer use. Mai Le serves as Haystack's Chief Executive Officer; she has equity interest in the company and serves on the company's board of directors.

Funding

This work was funded through NIH/NINDS Grant 1R41NS112029-01A1.

ABSTRACT

Introduction/Aims: Needle impedance-electromyography (iEMG) is a diagnostic modality currently under development that combines intramuscular electrical impedance with concentric electromyography (EMG) in a single needle. We designed, manufactured, and tested a prototype iEMG needle in a cohort of wild-type (WT) and SOD1G93A ALS mice to assess its ability to record impedance and EMG data.

Methods: A 6-electrode, 26-gauge, iEMG needle was designed and manufactured using a novel metallic weaving technique. Quantitative impedance and qualitative "gestalt" EMG were performed sequentially on bilateral quadriceps of 16-week-old SOD1G93A ALS (N=6) and WT (N=6) mice by connecting the needle first to an impedance analyzer (with the animal at rest) and then to a standard EMG system (with the animal fully under anesthesia to measure spontaneous activity and briefly during awakening to measure voluntary activity). The needle remained in the muscle throughout the measurement period.

Results: EMG data was qualitatively similar to that observed with a commercially-available concentric EMG needle; fibrillation potentials were observed in 84% of the ALS mice and none of the WT mice; motor unit potentials were also readily identified. Impedance data revealed significant differences in resistance, reactance, and phase values between the two groups, with ALS animals having reduced reactance and resistance values.

Discussion: This work demonstrates the feasibility of a single iEMG needle conforming to standard dimensions of size and function. Further progress of iEMG technology for enhanced neuromuscular diagnosis and quantification of disease status is currently in development.

Key Words: needle impedance-electrical impedance myography, ALS

INTRODUCTION

Since 1915, when Langley and Kato first described fibrillation potentials in muscle,[1] the mainstay of electrodiagnosis has relied upon assessment of the *active* properties of the myofiber membranes. However, standard needle electromyography (EMG) is insensitive to alterations in the (passive) volume electrical conduction properties of the muscle tissue since it measures only active depolarizations and repolarizations of myofibers. Despite electrical impedance studies being pioneered at around the same time period,[2] the two technologies have remained separate. One approach of measuring these volume conduction properties is by measuring simultaneously EMG and electrical impedance of the muscle tissue using a single needle.[3,4] This is the fundamental principle of needle impedance EMG (iEMG). With virtually the same clinical effort as EMG, impedance values obtained during an iEMG test could complement EMG data by providing insight into the composition and architecture of the muscle volume altered in many neuromuscular disorders (NMDs), and not available in EMG, including information on the degree of fibrosis,[5] fatty infiltration,[6] edema,[7] and even myofiber size and distribution.[8] Moreover, alterations in the impedance during active contraction could provide yet another window into the ramifications of disease on muscle function.[9]

With input from computer simulations, we first designed and then built a 5-electrode 19-gauge iEMG needle to demonstrate the potential of performing both impedance (4 electrodes) and EMG (1 electrode with external ground and reference electrodes) using a single needle,[10] which we used to study a small group of wild-type and muscular dystrophy mice.[11] Although limited, the data gathered provided initial useful proof-of-principle support for the concept of iEMG. Since then, we have performed several studies to further develop the science around the iEMG concept, including modeling a potential imaging needle[12] and mathematical studies for measuring the electrical properties of muscle.[13] Recently, we utilized two commercial concentric needles, separated by a consistent distance and inserted simultaneously to perform four-electrode impedance measurements in patients with a variety of NMDs.[14] All of these studies led us to

design a 26-gauge iEMG needle with dimensions similar to those of a standard EMG needle used in regular clinical practice.

Now, we take this work a step further by using advanced engineering techniques to develop, manufacture, and test a 26-gauge 6-electrode iEMG needle that can perform concentric needle EMG recordings and impedance measurements. Here, we present early data using this needle, assessing its impedance recording characteristics in saline solution and then evaluating its performance measuring impedance and EMG in a group of wild-type (WT) and SOD1G93A ALS mice.

METHODS

Needle iEMG fabrication

The prototype iEMG needle was provided by Haystack Diagnostics, Inc (Lowell, MA). It is a 26-gauge needle configured with 2 EMG electrodes and 4 impedance electrodes made of stainless steel (Figure 1). The needle was configured with a connector that had six color-coded leads (see Figure 1B), 2 leads for the EMG electrodes, and 4 for the impedance electrodes, such that the impedance and EMG measurement systems could be attached with alligator clips to these individual leads.

Recording characteristics of the iEMG needle

We performed a set of test measurements in air and saline solution to characterize the electrodes' contact impedance using 3 different iEMG needles. Each iEMG needle was held by a grounded micromanipulator and then the electrodes' contact impedance measured using a reference impedance analyzer (E4990A, Keysight, Santa Rosa, CA) including impedance magnitude, resistance, phase, and capacitance between the cannula and inner core of the electrodes. Then, we immersed the iEMG needle into 0.9% saline solution at room temperature and impedance data was recorded after ensuring electrode stabilization.

Animals

All experimental procedures were approved by the Institutional Animal Care and Use Committee at Beth Israel Deaconess Medical Center. Breeding pairs of ALS B6SJL-Tg(SOD1-G93A)1Gur/J mice were obtained from Jackson Laboratories (Bar Harbor, ME, USA) and bred to obtain 6 ALS animals (5 male and 1 female) that were used in these analyses. Six additional WT animals (5 male and 1 female) were also used. All animals were fed standard chow *ad libitum* up until the time of study when the animals were approximately 16-18 weeks of age. During the experiment, the animals were anesthetized with isoflurane (0.5%–3%) delivered by a nosecone.

In vivo needle iEMG

Impedance and EMG measurements were performed sequentially without removing the needle from the muscle. Impedance measurements were made with the mView impedance system (Myolex Inc., Boston, MA) interfaced to the iEMG needle connector (Figure 1). The impedance device was configured to measure R and X values at 31 logarithmically spaced frequencies from 1 kHz to 1 MHz.

With the animal under deep anesthesia, the fur overlying the quadriceps bilaterally was removed with a standard rechargeable clipper. To facilitate the iEMG needle insertion without bending the needle or damaging the skin, a small hole was then placed in the skin using a 21-gauge angiocath needle just proximal to the left knee. The iEMG needle was then passed through the hole into the center of quadriceps with an effort to keep the needle parallel to the long axis of the muscle so that all 6 electrodes remained within the muscle itself. Once situated, a first set of measurements was made. The needle was then partially withdrawn and then reinserted and a second set of measurements obtained.

Once the impedance data was collected, the Natus Ultrapro S100 EMG system with Synergy Software (Natus Neuro, Middleton WI) was then connected to the EMG leads on the

needle and an adhesive ground electrode was placed on the tail. With the animal still under deep anesthesia, small movements of the electrode were made and the EMG activity recorded. Once several insertions of the needle were completed and 20 seconds of spontaneous activity recorded, the anesthesia was lightened to the point that voluntary movement of the animal could be observed. EMG activity was briefly collected and qualitatively assessed and the needle removed quickly as the animal regained full consciousness. The impedance and EMG procedures were then repeated on the right quadriceps in identical fashion.

Impedance data was directly exported from the system for analysis. Similarly, the EMG data from the evaluation of the spontaneous activity was exported as a text file. These were then reconstructed into a single 20 second trace and de-identified as to specific animal and its disease status.

Statistical analyses

Since a multi-frequency impedance measurement provides quantitative values, standard unpaired t-tests (two-tailed, significance $p < 0.05$) of R, X and phase (= arctan X/R) values at 50 kHz were calculated to compare impedance differences between the wild-type and ALS mice. For reproducibility analyses, standard intra-class correlation coefficients (ICCs) were calculated.

The spontaneous activity was graded in a blinded fashion based on the absence or presence of fibrillation potentials as being likely WT or likely ALS, respectively. The voluntary activity data, recorded briefly as the animal regained consciousness, were only qualitatively assessed since there was insufficient data to perform any formal quantitative motor unit potential (MUP) evaluation.

RESULTS

Electrode characterization results. Table 1 summarizes the electrode recording characteristics of 3 different iEMG needles in air and then immersed in an ungrounded saline

bath. At 10 kHz, the contact impedance is only 1 kOhm (decreasing with increasing frequency), which ensures a good electrical contact for measuring biopotential signals such as EMG.

Needle iEMG can detect spontaneous and voluntary EMG activity in ALS and WT mice. There was a total of 19 usable EMG traces (9 ALS and 10 WT) from the two sides out of a total of 23 muscles recorded (1 animal had only one side measured and 3 traces had excessive 60 Hz interference or were otherwise technically limited). The blinded analysis of the individual 19 quadriceps spontaneous activity yielded 16 correctly identified and 3 misidentified (84.2% accuracy) as ALS or WT based on the presence of fibrillation potentials alone (see Figure 2 for example of fibrillation potentials observed). The 3 animals that were misclassified were all ALS animals in which no fibrillation potentials were observed. In secondary review of the traces, no fibrillation potentials were apparent even with the knowledge that these animals had ALS, suggesting that these were simply false negative animals (possibly secondary to reduced transgene copy number).

Voluntary activity, recorded as the animals regained consciousness, revealed readily identifiable MUPs in both ALS and WT animals, but the activity was too briefly assessed to perform any form of quantitative or qualitative analysis. An example of the voluntary data from an ALS animal is shown in Figure 2B.

Needle iEMG multifrequency impedance values show characteristic features from ALS and healthy WT muscle. Figure 3 shows average (± 95% confidence interval based on Loess regression) for resistance, reactance, and Phase values in WT and ALS mice. There is reduced resistance across the frequency spectrum in ALS, especially at low frequencies. This reduction in resistance is likely due to increased free water in the muscle, similar to that observed on MRI of denervated muscle.[15] Myofiber membrane integrity changes are also reflected in reduced reactance in ALS, where myofiber atrophy and denervation impact the ability of the tissue to store electrical charge.

Single-frequency impedance differences and reproducibility. Figure 4 shows single-frequency 50 kHz resistance, reactance, and phase data, revealing significant differences between groups (showing median and interquartile range in box plot). In addition, Figure 5 shows the ICC values supporting the high reproducibility of the technique.

DISCUSSION

In this work, we measured impedance and EMG sequentially as we do not have a system capable of performing such measurements concurrently. Being able to measure both impedance and EMG simultaneously would not only speed data collection but may also provide new insights as to how EMG activity is related to muscle impedance changes. For example, it potentially could show us that one region of muscle with substantial fibrillation potentials also has a relatively low resistance—supporting the concept that denervated myofibers become "leaky" and more capable of conducting electrical current.[16] It may also help reveal the relationship between MUP size and impedance change. Undoubtedly, this will be a very complex relationship since impedance not only has the potential for detecting the opening and closing of ion channels but will also be impacted by the physical alteration in shape as myofibers contract. Nevertheless, we anticipate that when the required hardware becomes available to measure simultaneously impedance and EMG, we may be able to expand neurophysiological skeletal muscle science in new directions.

From a practical standpoint, iEMG needle technology could offer electrodiagnostic (EDX) medicine specialists several advantages over standard EMG. First, sensing impedance as the needle is inserted into the muscle could help ensure that the needle is positioned appropriately within the muscle and not in subcutaneous tissue or fascia. Whereas electromyographers are generally practiced in knowing when they are in the muscle based on the presence of clear insertional activity with needle movement, this additional feature available with iEMG technology will likely be able to improve the needle insertion process and provide physicians additional confidence in needle placement. Second, it will provide an instantaneous measure of the volume

conduction properties of the muscle tissue. It is true that today, electromyographers would not know how to interpret these values or their frequency dependence. However, in the future, we foresee that normative volume conduction values could be established that could provide insight into the composition of the tissue —including its degree of fibrosis, fatty infiltration or edema— and use this new information to track disease progression or therapeutic treatment. Third, and perhaps most intriguingly, we will explore the use of machine learning approaches to combine both impedance and EMG data sets and assist the EDX medicine specialist to improve diagnostic outcomes, disease severity assignment and measurement of muscle specific force.

This work is restricted to animals and therefore has limitations. In assessing mice, we studied a single large muscle group and were restricted to mainly studying spontaneous / insertional activity and not the MUP morphology or recruitment patterns. Second, the impedance and EMG data was assessed sequentially and not simultaneously. Third, we did not study a myopathic condition or the impact of chronicity on the data (i.e., comparing acute versus chronic injury) . Fifth, we did not compare different iEMG needles.

Despite these limitations, this study represents a major step forward in developing needle iEMG technology. Here, we were able to create an iEMG needle that conforms to the standard size of commercially available EMG needles capable of obtaining intramuscular impedance and concentric EMG data, which in our view, represents a substantial technological milestone in modernizing EMG. It also demonstrates that we can readily identify differences between healthy and diseased muscle. Given the potential for substantially expanding the information obtained regarding muscle condition with the needle examination, further development of iEMG as a tool for general EDX medicine specialists use is being pursued.

REFERENCES

1. Langley JN, Kato T. The physiological action of physostigmine and its action on denervated skeletal muscle. *J Physiol* 1915;**49**.
2. Hemingway A, McClendon JF. THE HIGH FREQUENCY RESISTANCE OF HUMAN TISSUE. *Am J Physiol Content* 1932;**102**.
3. Rutkove SB, Sanchez B. Electrical impedance methods in neuromuscular assessment: An overview. *Cold Spring Harb Perspect Med* 2019;**9**.
4. Sanchez B, Rutkove SB. Electrical Impedance Myography and Its Applications in Neuromuscular Disorders. *Neurotherapeutics* 2017;**14**:107–118.
5. Pandeya SR, Nagy JA, Riveros D, Semple C, Taylor RS, Mortreux M *et al.* Estimating myofiber cross-sectional area and connective tissue deposition with electrical impedance myography: A study in D2-mdx mice. *Muscle Nerve* 2021;**63**:941–950.
6. Pandeya SR, Nagy JA, Riveros D, Semple C, Taylor RS, Mortreux M *et al.* Predicting myofiber cross-sectional area and triglyceride content with electrical impedance myography: A study in db/db mice. *Muscle and Nerve* 2020 doi:10.1002/mus.27095.
7. Mortreux M, Semple C, Riveros D, Nagy JA, Rutkove SB. Electrical impedance myography for the detection of muscle inflammation induced by λ-carrageenan. *PLoS One* 2019;**14**.
8. Kapur K, Nagy JA, Taylor RS, Sanchez B, Rutkove SB. Estimating myofiber size with electrical impedance myography: a study in amyotrophic lateral sclerosis mice. *Muscle Nerve* 2018;**58**:713–717.
9. Sanchez B, Li J, Geisbush T, Bardia RB, Rutkove SB. Impedance Alterations in Healthy and Diseased Mice During Electrically Induced Muscle Contraction. *IEEE Trans Biomed Eng* 2016;**63**:1602–1612.
10. Kwon H, Rutkove SB, Sanchez B. Recording characteristics of electrical impedance myography needle electrodes. *Physiol Meas* 2017;**38**:1748–1765.
11. Kwon H, Di Cristina JF, Rutkove SB, Sanchez B. Recording characteristics of electrical

impedance-electromyography needle electrodes. *Physiol Meas* 2018;**39**:055005.

12. Rutkove SB, Kwon H, Guasch M, Wu JS, Sanchez B. Electrical impedance imaging of human muscle at the microscopic scale using a multi-electrode needle device: A simulation study. *Clin Neurophysiol* 2018;**129**:1704–1708.
13. Kwon H, Nagy JA, Taylor R, Rutkove SB, Sanchez B. New electrical impedance methods for the in situ measurement of the complex permittivity of anisotropic biological tissues. *Phys Med Biol* 2017;**62**.
14. Cardoner MM de M, Kwon H, Pulido HVG, Nagy J, Rutkove S, Sanchez B. Modeling and Reproducibility of Twin Concentric Electrical Impedance Myography. *IEEE Trans Biomed Eng* 2021;**68**:3068–3077.
15. Kamath S, Venkatanarasimha N, Walsh MA, Hughes PM. MRI appearance of muscle denervation. *Skelet Radiol* 2008;**37**:397–404.
16. Sanchez B, Rutkove SB. Present Uses, Future Applications, and Technical Underpinnings of Electrical Impedance Myography. *Curr Neurol Neurosci Rep* 2017;**17**:86.

ABBREVIATIONS

ALS, amyotrophic lateral sclerosis

EMG, electromyography

ICC, intra-class correlation coefficients

iEMG, needle impedance-electromyography

kHz, kiloHertz

MHz, megaHertz

MUP, motor unit potential

mV, millivolts

NMD, neuromuscular disorders

WT**,** wild type

FIGURE LEGENDS

Figure 1. Overview of the iEMG needle. The EMG electrodes were concentric in design with the E1 tungsten electrode within the beveled tip of the needle within a core that is electrically isolated from the remainder of the needle. The E2 stainless steel electrode was of standard design in that it surrounded the tungsten tip electrode concentrically and was electrically isolated from it. However, unlike standard concentric EMG needles, the E2 electrode did not extend up the entire shaft of the electrode and was only 2 mm in length to allow for the placement of impedance electrodes. The 4 ring impedance electrodes were placed along the shaft of the needle, each of 1 mm in length with 0.5 mm separation between the electrodes' edge to edge, and 0.5 mm away from the E2 EMG electrode.

Figure 2. Examples of EMG data collected with the iEMG needle. **A.** Fibrillation potential in ALS mouse; **B.** Motor unit potentials in ALS mouse.

Figure 3. Impedance data overview. Average resistance, reactance and phase multi-frequency curves from all animals measured; blue area represents 95% confidence interval based on Loess regression**.**

Figure 4. Comparison of 50 kHz resistance, reactance and phase values comparing WT and ALS mice. Median values and 25%-75% interquartile range shown.

Figure 5. Reproducibility of measurements after a small movement of the needle; intraclass correlation coefficients (ICCs) reported.

TABLE CAPTION

Table 1. Impedance characterization of impedance electrodes available in the iEMG needle measured at 10 kHz measured with a voltage amplitude of 50 mV.

	AIR				SALINE SOLUTION			
Impedance Electrodes	**Impedance magnitude (kiloOhm)**	**Phase (degrees)**	**Resistance (kiloOhm)**	**Capacitance (picoFarads)**	**Impedance Magnitude (kiloOhm)**	**Phase (degrees)**	**Resistance (kiloOhm)**	**Capacitance (nanoFarads)**
iEMG Needle 1	466	-86	32.50	34.23	0.8	-22	0.74	53.10
iEMG Needle 2	399	-86	27.83	39.98	1	-21	0.93	44.41
iEMG Needle 3	399	-86	27.83	39.98	0.6	-17	0.57	90.72
Mean	421.33	-86	29.39	38.06	0.8	-20	0.75	62.74
STD	38.68	0	2.70	3.32	0.2	2.64	0.18	24.61

A

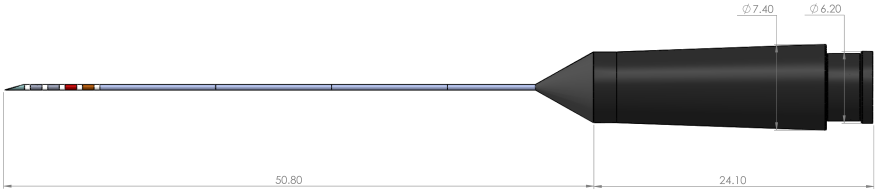

B

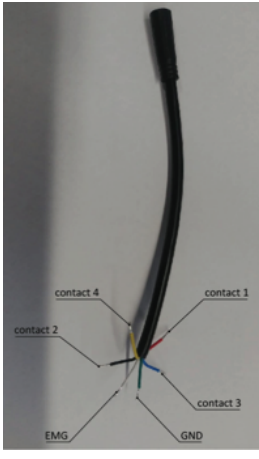

CONTACTS DIMENSIONS

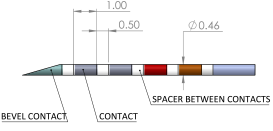

ELECTRODE LAYERS

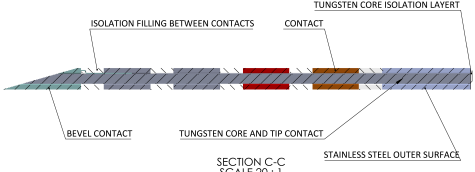

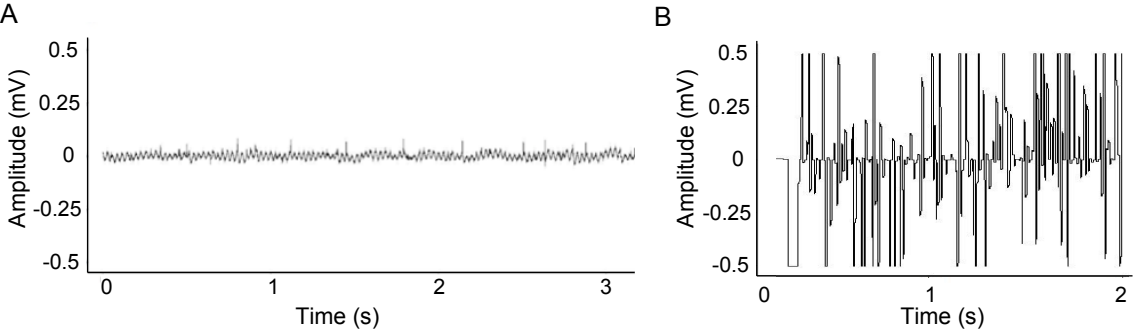
A
0.5
0.25
0
-0.25
-0.5
Amplitude (mV)
0
1
2
3
Time (s)
B
0.5
0.25
0
-0.25
-0.5
Amplitude (mV)
0
1
2
Time (s)

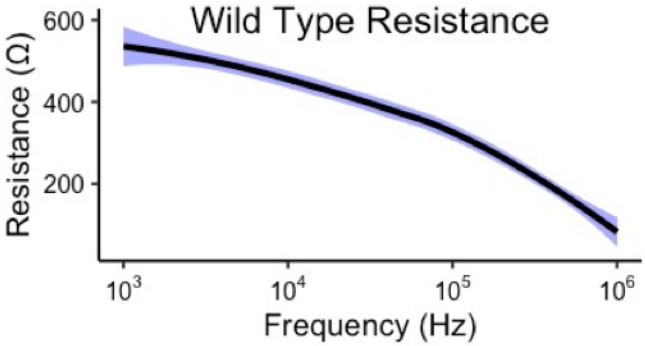
Wild Type Resistance
Resistance (Ω)
600
400
200
10^3
10^4
10^5
10^6
Frequency (Hz)

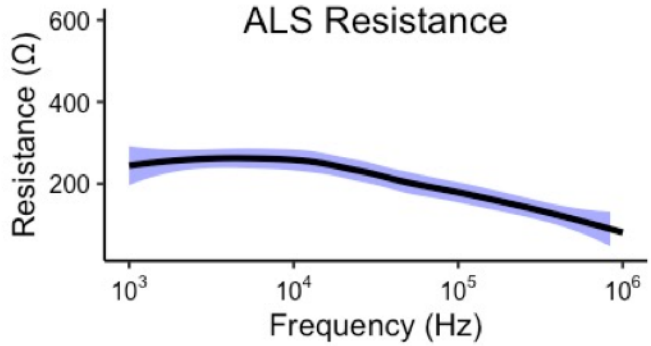
ALS Resistance
Resistance (Ω)
600
400
200
10^3
10^4
10^5
10^6
Frequency (Hz)

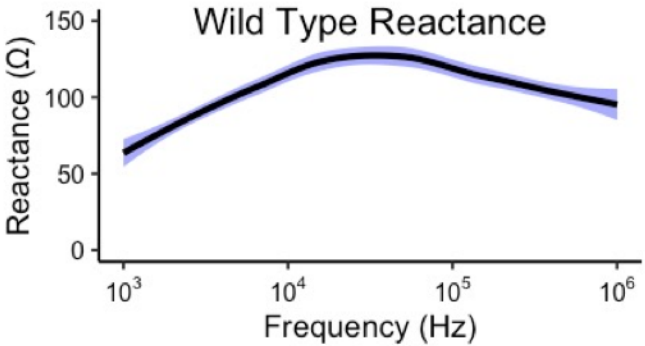
Wild Type Reactance
Reactance (Ω)
150
100
50
0
10^3
10^4
10^5
10^6
Frequency (Hz)

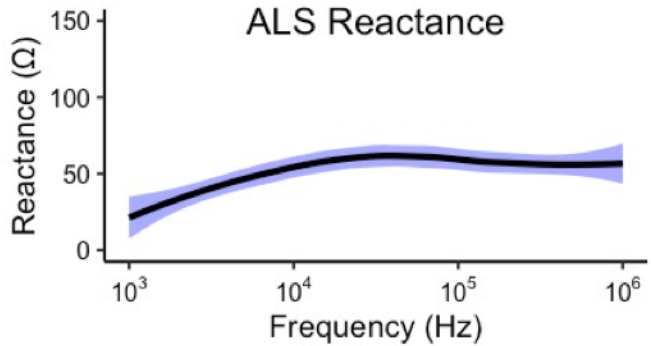
ALS Reactance
Reactance (Ω)
150
100
50
0
10^3
10^4
10^5
10^6
Frequency (Hz)

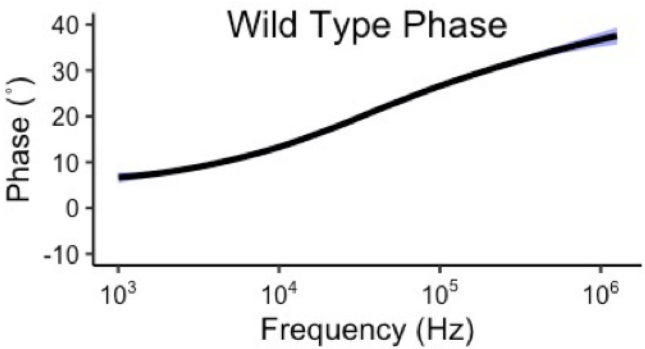
Wild Type Phase
Phase (°)
40
30
20
10
0
-10
10^3
10^4
10^5
10^6
Frequency (Hz)

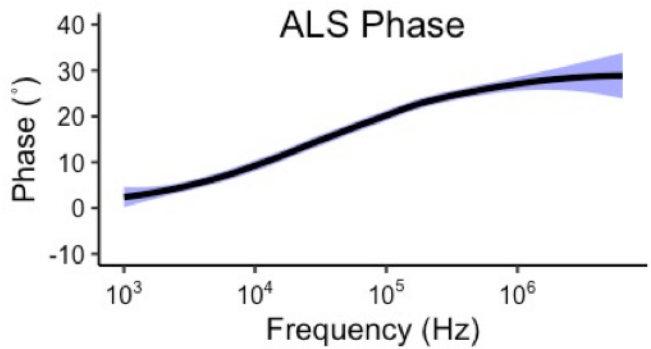
ALS Phase
Phase (°)
40
30
20
10
0
-10
10^3
10^4
10^5
10^6
Frequency (Hz)

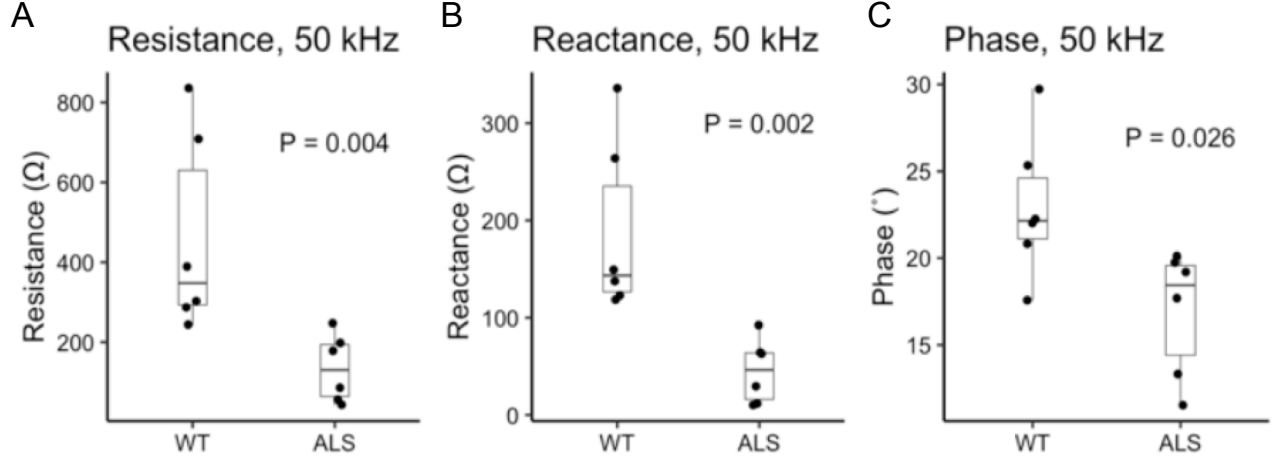
A
Resistance, 50 kHz
Resistance (Ω)
800
600
400
200
P = 0.004
WT
ALS
B
Reactance, 50 kHz
Reactance (Ω)
300
200
100
0
P = 0.002
WT
ALS
C
Phase, 50 kHz
Phase (°)
30
25
20
15
P = 0.026
WT
ALS

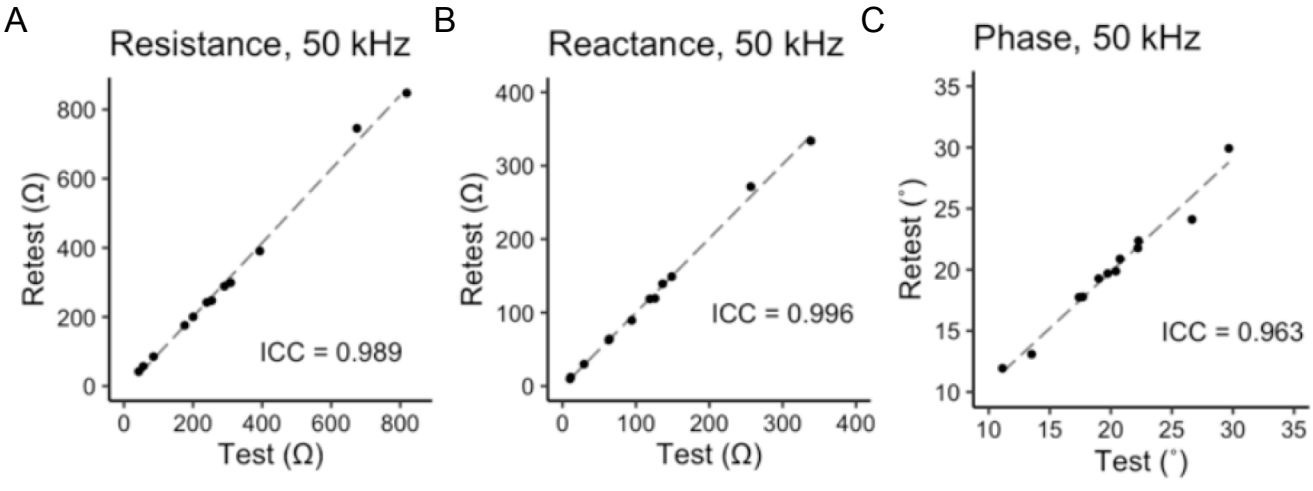
A
Resistance, 50 kHz
Retest (Ω)
Test (Ω)
ICC = 0.989
0
200
400
600
800
B
Reactance, 50 kHz
Retest (Ω)
Test (Ω)
ICC = 0.996
0
100
200
300
400
C
Phase, 50 kHz
Retest (°)
Test (°)
ICC = 0.963
10
15
20
25
30
35